



HAL
open science

Angular dependence of tunnel magnetoresistance in magnetic tunnel junctions and specific aspects in spin-filtering devices

François Montaigne, C. Tiusan, Michel Hehn

► **To cite this version:**

François Montaigne, C. Tiusan, Michel Hehn. Angular dependence of tunnel magnetoresistance in magnetic tunnel junctions and specific aspects in spin-filtering devices. *Journal of Applied Physics*, 2010, 108 (6), pp.063912. 10.1063/1.3466778 . hal-04370057

HAL Id: hal-04370057

<https://hal.science/hal-04370057v1>

Submitted on 1 Aug 2024

HAL is a multi-disciplinary open access archive for the deposit and dissemination of scientific research documents, whether they are published or not. The documents may come from teaching and research institutions in France or abroad, or from public or private research centers.

L'archive ouverte pluridisciplinaire **HAL**, est destinée au dépôt et à la diffusion de documents scientifiques de niveau recherche, publiés ou non, émanant des établissements d'enseignement et de recherche français ou étrangers, des laboratoires publics ou privés.

RESEARCH ARTICLE | SEPTEMBER 22 2010

Angular dependence of tunnel magnetoresistance in magnetic tunnel junctions and specific aspects in spin-filtering devices


F. Montaigne; C. Tiusan; M. Hehn




J. Appl. Phys. 108, 063912 (2010)

<https://doi.org/10.1063/1.3466778>







Nanotechnology & Materials Science




Optics & Photonics



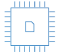
Impedance Analysis




Scanning Probe Microscopy



Sensors




Failure Analysis & Semiconductors



Unlock the Full Spectrum.
From DC to 8.5 GHz.
Your Application. Measured.

[Find out more](#)



Angular dependence of tunnel magnetoresistance in magnetic tunnel junctions and specific aspects in spin-filtering devices

F. Montaigne,^{a)} C. Tiusan, and M. Hehn

Institut Jean Lamour, Nancy-Université, CNRS, boulevard des aiguillettes, BP 329, F-54506 Vandoeuvre lès Nancy, France

(Received 11 March 2010; accepted 23 June 2010; published online 22 September 2010)

We propose a general formalism to describe accurately the angular dependence of the magnetoresistance. A parabolic band model is used to determine without approximation the conductance of arbitrary complex heterostructures. Simple analytical expressions are obtained in some limit cases. Particularly, we show that significant deviation from the cosine dependence is expected for ferromagnetic barriers. Numerical computations are used to quantify the deviation from the cosine dependence for normal and ferromagnetic barriers and support the precedent conclusion. Finally, the influence of the applied voltage on the angular dependence of magnetoresistance is discussed. © 2010 American Institute of Physics. [doi:10.1063/1.3466778]

I. INTRODUCTION

The electronic transport in magnetic tunnel junctions (MTJs) is modulated by the external magnetic field which induces changes in the magnetization configuration of the two ferromagnetic electrodes separated by the thin tunnel insulating barrier. This defines the tunnel magnetoresistance (TMR) effect which leads nowadays to large scale applications of MTJs in sensors and data storage devices.¹ The rapid development of this topic over the last decade is marked by a rapid evolution of the level of TMR. Indeed from a 10% TMR at room temperature in amorphous aluminum oxide barrier-based MTJ in 1995, it gets now beyond 600% in crystalline MgO barrier MTJ.²⁻⁷ Beyond the interest of the TMR amplitude enhancement for MTJs with smaller and smaller area resistance for high density storage applications, new research directions emerge.

Typically, the magnetoelectric properties of MTJs are often analyzed in terms of parallel (P) and antiparallel (AP) configurations of the magnetizations. The TMR amplitude defines the relative difference of resistance between the P and AP states. However noncollinear configuration of the magnetizations can lead to interesting new and specific phenomena.⁸ One of the best examples concerns the spin torque induced by a spin polarized current torque theoretically predicted by Berger⁹ and Slonczewski.¹⁰ The efficiency of spin torque is higher for noncollinear configurations of the magnetization. Moreover noncollinear configurations are observed in precessional regimes excited by spin transfer. As the interest for noncollinear configurations of the magnetizations increases, it appears necessary to pay more attention to the angular dependence of the magnetoresistive effects.

Urazhdin *et al.*¹¹ have studied the angular dependence of giant magneto resistance in spin-valves in current-in-plane geometry. They have shown that the angular dependence can be accurately fitted to the following expression:

$$R(\theta) = R(0) + \Delta R \frac{1 - \cos \theta}{2 + \chi(1 + \cos \theta)}, \quad (1)$$

where χ is a fitting parameter and θ is the relative angle of magnetizations in the ferromagnetic layers.

This expression was established within the framework of a two series resistor model for a symmetric spin valve system.¹² It has been extended to multilayers with noncollinear magnetization and it appears that the angular dependence of the giant magnetoresistance (GMR) provides information on the spin currents in the ferromagnetic layers.¹¹ These experiments allowed to measure the transverse spin-current penetration length in the ferromagnets and to correlate the angular dependence of the GMR to the spin torque.

Concerning the angular dependence of the TMR in ferromagnetic/insulator/ferromagnetic structures, it is generally admitted that the conductance has a purely cosine dependence. This has been shown theoretically by Slonczewski¹³ within a parabolic band model in the low transmission limit (large resistance tunnel junctions). This angular dependence of the TMR has been verified experimentally by Jaffrès *et al.* in Ref. 14, in the low transmission and low field regime, for AlO_x based MTJs with Co magnetic electrodes having an intrinsic area resistance of $2.5 \times 10^8 \Omega \mu\text{m}^2$.

Recently, another interesting phenomenon, the anisotropic tunneling magnetoresistance (TAMR), has been reported in tunnel junctions with transition metal electrodes and with both MgO and AlO_x barriers.¹⁵ It concerns an unusual angular dependence of the TMR. When the magnetization is turned out from an in plane to a perpendicular to plane configuration by sufficiently large fields to keep both magnetizations parallel, a complex angular dependence of the tunneling resistance is measured with twofold and fourfold components which vary strongly with the bias voltage. In these systems, the TAMR effect originates from the spin-orbit coupling which induces anisotropy of the bulk and interface density of states with respect to the magnetization direction, with a strong influence of the interface resonant states of ferromagnetic electrodes.¹⁶

^{a)}Electronic mail: francois.montaigne@lpm.u-nancy.fr.

Other particular angular dependences have also been predicted in quantum dot systems attached to ferromagnetic leads.^{17–19} Here, the angular dependence reflects the complex interplay between magnetoresistance (MR), spin accumulation, and spin precession.

Within all these different topics related to angular dependence of the TMR, one important regime remained yet insufficiently explored: the large tunneling transmission limit corresponding to low resistance tunnel junctions. This regime has a large interest both for read-heads technology and high density magnetic memory integration. Significant deviations from the low transparency limit approach have been already predicted for tunneling characteristics in MTJs with collinear magnetization, in one of our previous work.²⁰ Therefore, in this regime the angular dependence of the tunnel resistance is worth to be carefully analyzed. On the other hand, no attention has been paid up to now to the angular dependence of the TMR in more complex structures, including for example quantum wells or ferromagnetic insulators.

In this article, we propose a general formalism to describe accurately the angular dependence of the MR without any approximation. This formalism is valid in any transmission regime. It considers arbitrary complex heterostructures within a parabolic band model for the tunneling. Our model leads to simple analytical expressions that can be obtained in some limit cases. Moreover, we show that significant deviation from the cosine dependence is expected in case of MTJs with ferromagnetic barriers. Numerical computations have been developed to quantify the deviation from the cosine dependence. Comparative analysis has been performed for MTJ systems with normal and ferromagnetic barriers. Beyond the standard P-AP conductance analysis giving the TMR amplitude, the angular dependence of magnetotransport provides supplementary information about the transport phenomena.

II. FORMALISM

The free-electron-like model considers the wave function of electrons as plane waves with parabolic energy bands. This approach has been particularly successful to describe semiconductor heterostructures like quantum wells or resonant tunneling diodes.²¹ Even if this simple parabolic band approach does not describe accurately the band structures of transition metals, it remains appropriate to study coherent effects in the tunnel current.²²

To determine the electron wave function, the heterostructure is divided in different regions in which the potentials vary linearly. In regions containing magnetic materials, different material parameters are used for the spin up and spin down bands. The Schrödinger equation is solved analytically in each region. The transmission probability is finally calculated using the continuity of the wave function and of the current probability.

Due to lateral invariance, the wave function is given by $\psi(\vec{r}) = \varphi(z) \cdot e^{i\vec{k}_\parallel \cdot \vec{r}_\parallel}$, z being the position along the heterostructure. In any region of the heterostructure without change in the quantification axis, the wave function for each spin direction $\varphi(z)$ and their derivative divided by the effective

mass $\varphi'(z)/m(z)$ are continuous. Between two arbitrary points, the linear combination between the previous quantities can be written as (see, Appendix)

$$\begin{pmatrix} \varphi^\uparrow(z_1) \\ \varphi^{\uparrow'}(z_1)/m^\uparrow(z_1) \\ \varphi^\downarrow(z_1) \\ \varphi^{\downarrow'}(z_1)/m^\downarrow(z_1) \end{pmatrix} = \begin{pmatrix} \alpha_\uparrow & \beta_\uparrow & 0 & 0 \\ \gamma_\uparrow & \delta_\uparrow & 0 & 0 \\ 0 & 0 & \alpha_\downarrow & \beta_\downarrow \\ 0 & 0 & \gamma_\downarrow & \delta_\downarrow \end{pmatrix} \times \begin{pmatrix} \varphi^\uparrow(z_2) \\ \varphi^{\uparrow'}(z_2)/m^\uparrow(z_2) \\ \varphi^\downarrow(z_2) \\ \varphi^{\downarrow'}(z_2)/m^\downarrow(z_2) \end{pmatrix}. \quad (2)$$

Note that the conservation of current probability imposes that the determinant of each submatrix ($\alpha_\sigma \delta_\sigma - \beta_\sigma \gamma_\sigma$) is equal to 1. Each submatrix is determined independently for each spin direction by solving the time independent Schrödinger equation. Values for simple potentials are provided in the Appendix. Values for complex potentials (heterostructures, gradients, etc.) can be determined by multiplication of elementary transfer matrix. For nonmagnetic regions (same band parameters for both spin direction) the two submatrixes are equal.

A change in the quantification axis (different directions of the magnetization in the MTJ ferromagnetic electrodes) is taking into account with the spinor relation. This relation has the general following form:

$$\begin{pmatrix} \varphi^\uparrow(z) \\ \varphi^{\uparrow'}(z) \\ m^\uparrow(z) \\ \varphi^\downarrow(z) \\ \varphi^{\downarrow'}(z) \\ m^\downarrow(z) \end{pmatrix} \Bigg|_{L \text{ axis}} = \begin{pmatrix} A & 0 & B & 0 \\ 0 & A & 0 & B \\ -\bar{B} & 0 & \bar{A} & 0 \\ 0 & -\bar{B} & 0 & \bar{A} \end{pmatrix} \times \begin{pmatrix} \varphi^\uparrow(z) \\ \varphi^{\uparrow'}(z) \\ m^\uparrow(z) \\ \varphi^\downarrow(z) \\ \varphi^{\downarrow'}(z) \\ m^\downarrow(z) \end{pmatrix} \Bigg|_{R \text{ axis}}, \quad (3)$$

with A and B two complex coefficients related by $|A|^2 + |B|^2 = 1$ (the determinant of this matrix is thus 1). Generally, the wave functions in the two electrodes are thus linked by a 4×4 complex matrix that results from the multiplication of several matrixes of type (2) and (3). This total transfer matrix has consequently a determinant of 1.

If we consider a spin up electron propagating from the left (L) to the right (R) electrode, the wave functions are given by

$$\begin{aligned}\varphi_L^\uparrow(z) &= e^{i k_L^\uparrow(z-z_L)} + R^\uparrow \cdot e^{-i k_L^\uparrow(z-z_L)} & \varphi_R^\uparrow(z) &= T^\uparrow \cdot e^{i k_R^\uparrow(z-z_R)} \\ \varphi_L^\downarrow(z) &= R^\downarrow \cdot e^{-i k_L^\downarrow(z-z_L)} & \varphi_R^\downarrow(z) &= T^\downarrow \cdot e^{i k_R^\downarrow(z-z_R)},\end{aligned}\quad (4)$$

k_L^\uparrow , k_L^\downarrow , k_R^\uparrow , and k_R^\downarrow being the real wave vector in the R and L electrode for up and down spins.

These wave functions are then related by the general matrix

$$\begin{pmatrix} 1 + R^\uparrow \\ \frac{i \cdot k_L^\uparrow}{m_L^\uparrow} (1 - R^\uparrow) \\ R^\downarrow \\ -R^\downarrow \frac{i \cdot k_L^\downarrow}{m_L^\downarrow} \end{pmatrix} = \begin{pmatrix} \alpha_{\uparrow\uparrow} & \beta_{\uparrow\uparrow} & \alpha_{\uparrow\downarrow} & \beta_{\uparrow\downarrow} \\ \gamma_{\uparrow\uparrow} & \delta_{\uparrow\uparrow} & \gamma_{\uparrow\downarrow} & \delta_{\uparrow\downarrow} \\ \alpha_{\downarrow\uparrow} & \beta_{\downarrow\uparrow} & \alpha_{\downarrow\downarrow} & \beta_{\downarrow\downarrow} \\ \gamma_{\downarrow\uparrow} & \delta_{\downarrow\uparrow} & \gamma_{\downarrow\downarrow} & \delta_{\downarrow\downarrow} \end{pmatrix} \times \begin{pmatrix} T^\uparrow \\ \frac{i \cdot k_R^\uparrow}{m_R^\uparrow} T^\uparrow \\ T^\downarrow \\ \frac{i \cdot k_R^\downarrow}{m_R^\downarrow} T^\downarrow \end{pmatrix}. \quad (5)$$

The resolution of this linear system gives the value of the wave functions coefficients and particularly

$$\begin{aligned}T^\uparrow &= -2i \frac{X_{\downarrow\downarrow}}{X_{\uparrow\uparrow} \cdot X_{\downarrow\downarrow} - X_{\downarrow\downarrow} \cdot X_{\uparrow\uparrow}} \frac{k_L^\uparrow}{m_L^\uparrow}, \\ T^\downarrow &= 2i \frac{X_{\downarrow\uparrow}}{X_{\uparrow\uparrow} \cdot X_{\downarrow\uparrow} - X_{\downarrow\downarrow} \cdot X_{\uparrow\uparrow}} \frac{k_L^\uparrow}{m_L^\uparrow},\end{aligned}\quad (6)$$

with

$$X_{\sigma\sigma'} = \gamma_{\sigma\sigma'} - \beta_{\sigma\sigma'} \frac{k_L^\sigma}{m_L^\sigma} \frac{k_R^{\sigma'}}{m_R^{\sigma'}} + i \left(\alpha_{\sigma\sigma'} \frac{k_L^\sigma}{m_L^\sigma} + \delta_{\sigma\sigma'} \frac{k_R^{\sigma'}}{m_R^{\sigma'}} \right). \quad (7)$$

The transmission coefficient for an up spin is given by the ratio of the transmitted probability current (for spin up and down) over the incident probability current ($\hbar(k_L^\uparrow/m_L^\uparrow)$)

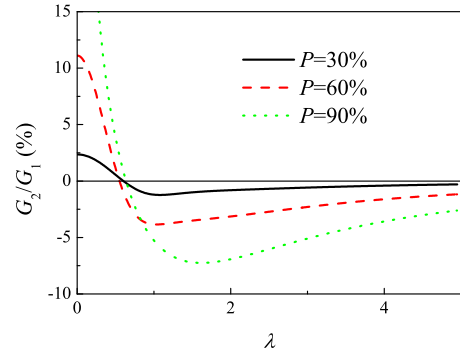


FIG. 1. (Color online) G_2/G_1 ratio for a Dirac barrier as a function of the barrier height for three different spin polarisations.

$$\begin{aligned}D_{\rightarrow}^\uparrow &= \frac{\hbar \frac{k_R^\uparrow}{m_R^\uparrow} |T^\uparrow|^2 + \hbar \frac{k_R^\downarrow}{m_R^\downarrow} |T^\downarrow|^2}{\hbar \frac{k_L^\uparrow}{m_L^\uparrow}} \\ &= 4 \frac{\frac{k_R^\uparrow}{m_R^\uparrow} |X_{\downarrow\downarrow}|^2 + \frac{k_R^\downarrow}{m_R^\downarrow} |X_{\downarrow\uparrow}|^2}{m_L^\uparrow |X_{\uparrow\uparrow} \cdot X_{\downarrow\uparrow} - X_{\downarrow\downarrow} \cdot X_{\uparrow\uparrow}|^2}.\end{aligned}\quad (8)$$

With this general formalism, it is possible to address the angular variation in the TMR in any structure.

III. LIMIT CASES

Let us first consider a system of two identical ferromagnetic electrodes which magnetizations form an angle θ separated by a nonmagnetic region (whatever is the form of its potential). In that case, the spinor matrix has a very simple expression and the total transfer matrix is real and can be expressed as

$$\begin{pmatrix} \cos \frac{\theta}{2} & 0 & \sin \frac{\theta}{2} & 0 \\ 0 & \cos \frac{\theta}{2} & 0 & \sin \frac{\theta}{2} \\ -\sin \frac{\theta}{2} & 0 & \cos \frac{\theta}{2} & 0 \\ 0 & -\sin \frac{\theta}{2} & 0 & \cos \frac{\theta}{2} \end{pmatrix} \begin{pmatrix} \alpha & \beta & 0 & 0 \\ \gamma & \delta & 0 & 0 \\ 0 & 0 & \alpha & \beta \\ 0 & 0 & \gamma & \delta \end{pmatrix}.$$

Let us consider the contribution to the current of one energy level. It is proportional to the sum of the transmission coefficients of both spin directions. In our specific case, it has the general form

$$\begin{aligned}G &= D_{\rightarrow}^\uparrow + D_{\rightarrow}^\downarrow \\ &= 8 \frac{\left(\frac{k^\uparrow}{m^\uparrow} + \frac{k^\downarrow}{m^\downarrow} \right)^2 \left[\gamma^2 + (\alpha^2 + \delta^2) \frac{k^\uparrow k^\downarrow}{m^\uparrow m^\downarrow} + \beta^2 \left(\frac{k^\uparrow k^\downarrow}{m^\uparrow m^\downarrow} \right)^2 \right] + 8 \left(\frac{k^\uparrow k^\downarrow}{m^\uparrow m^\downarrow} \right)^2 + \left[\gamma^2 - (\alpha^2 + \delta^2) \frac{k^\uparrow k^\downarrow}{m^\uparrow m^\downarrow} + \beta^2 \left(\frac{k^\uparrow k^\downarrow}{m^\uparrow m^\downarrow} \right)^2 \right] \left(\frac{k^\uparrow}{m^\uparrow} - \frac{k^\downarrow}{m^\downarrow} \right)^2 \cos \theta}{4(\alpha + \delta)^2 \left(\frac{k^\uparrow}{m^\uparrow} + \frac{k^\downarrow}{m^\downarrow} \right)^2 \left(\gamma - \beta \frac{k^\uparrow k^\downarrow}{m^\uparrow m^\downarrow} \right)^2 + T_1^2 + 2T_1 \left(\frac{k^\uparrow}{m^\uparrow} - \frac{k^\downarrow}{m^\downarrow} \right)^2 \cos \theta + \left(\frac{k^\uparrow}{m^\uparrow} - \frac{k^\downarrow}{m^\downarrow} \right)^4 \cos^2 \theta},\end{aligned}\quad (9)$$

with $T_1 = 2[\gamma^2 + \beta^2(k^\uparrow/m^\uparrow)^2(k^\downarrow/m^\downarrow)^2 - (\alpha^2 + \delta^2)(k^\uparrow/m^\uparrow)(k^\downarrow/m^\downarrow)] - (\alpha\delta + \beta\gamma)(k^\uparrow/m^\uparrow + k^\downarrow/m^\downarrow)^2$.

This general angular dependence is therefore much more complex than that of a pure cosine. As the expression is quite complicated, we will first deal with simple cases.

If we consider an absence of barrier (direct contact between the two electrodes), $\alpha = \delta = 1$, $\beta = 0$, and $\gamma = 0$ and then G reduces to

$$G = 16 \frac{\frac{k^\uparrow k^\downarrow}{m^\uparrow m^\downarrow}}{\frac{k^{\uparrow 2}}{m^{\uparrow 2}} + 6 \frac{k^\uparrow k^\downarrow}{m^\uparrow m^\downarrow} + \frac{k^{\downarrow 2}}{m^{\downarrow 2}} - \left(\frac{k^\uparrow}{m^\uparrow} - \frac{k^\downarrow}{m^\downarrow} \right)^2 \cos \theta} = 4 \frac{1 - P^2}{2 - P^2 - P^2 \cos \theta}, \quad (10)$$

where $P = (k^\uparrow/m^\uparrow - k^\downarrow/m^\downarrow)/(k^\uparrow/m^\uparrow + k^\downarrow/m^\downarrow)$ is the intrinsic polarization of the electrode.

In that limit case, it is the resistance (and not the conductance) which has a cosine dependence [$\chi = 0$ in expression (1)].

Another simple case is the one of the δ barrier of the form $V(z) = (\hbar^2/2)\gamma \cdot \delta(z)$. This form of potential can be used for general modeling of interfacial scattering or tunnel barrier. It has been used in superconducting heterostructures,²³ ferromagnetic/insulator heterostructures,^{24,25} or spin injection in semiconductors.²⁶

Using the simple expression of transfer matrix associated to the δ barrier (see Appendix), the contribution to the current is given by

$$G = 4 \frac{2 + \lambda^2 - 3P^2 + P^4 - (1 - \lambda^2 - P^2)P^2 \cos \theta}{\lambda^4 + 2\lambda^2(2 + P^2) + (2 - P^2)^2 - 2(2 - \lambda^2 - P^2)P^2 \cos \theta + P^4 \cos^2 \theta}, \quad (11)$$

with $\lambda = \sqrt{2} \cdot \gamma / (k^\uparrow/m^\uparrow + k^\downarrow/m^\downarrow)$ which is related to the ‘‘height’’ of the barrier. In order to analyze quantitatively the deviation from the pure cosine dependence, it is convenient to use a Fourier decomposition of the angular dependence of the form

$$G(\theta) = G_0 + G_1 \cos \theta + G_2 \cos 2\theta + G_3 \cos 3\theta + \dots \quad (12)$$

The deviation from the pure cosine can thus be quantified by the G_2/G_1 ratio. Figure 1 represents this ratio for different spin polarizations as a function of the barrier height. If the deviation from the pure cosine is significant for low barrier, it decreases as the transmission of the barrier decreases. In the limit, of high barrier, the angular dependence is purely cosine [$g = 4(1 + P^2 \cos \theta)/\lambda^2$]. The deviation from the pure cosine increases with the polarization of the electrodes.

These conclusions are quite general and hold also for more complex barrier.

Let us now consider a classic rectangular barrier. The transfer matrix has the following form (see Appendix)

$$\begin{pmatrix} \alpha & \beta \\ \gamma & \delta \end{pmatrix} = \begin{pmatrix} \cosh(q \cdot d) & -\frac{m}{q} \sinh(q \cdot d) \\ -\frac{q}{m} \sinh(q \cdot d) & \cosh(q \cdot d) \end{pmatrix}. \quad (13)$$

The exact angular dependence deduced from this matrix is complicated and does not provide significant physical insight. This aspect will then be studied numerically in Sec. IV. The high attenuation limit ($q \cdot d \gg 1$) is often considered. In this approximation, only leading terms in $e^{q \cdot d}$ are significant and

$$G = 8 \frac{\left(\frac{k^\uparrow}{m^\uparrow} + \frac{k^\downarrow}{m^\downarrow} \right)^2 \left(\frac{k^\uparrow k^\downarrow}{m^\uparrow m^\downarrow} + \frac{q^2}{m^2} \right)^2 + \left(\frac{k^\uparrow}{m^\uparrow} - \frac{k^\downarrow}{m^\downarrow} \right)^2 \left(\frac{k^\uparrow k^\downarrow}{m^\uparrow m^\downarrow} - \frac{q^2}{m^2} \right)^2 \cos \theta}{\left(\frac{k^{\uparrow 2}}{m^{\uparrow 2}} + \frac{q^2}{m^2} \right)^2 \left(\frac{k^{\downarrow 2}}{m^{\downarrow 2}} + \frac{q^2}{m^2} \right)^2} \frac{q^2}{m^2} e^{-2q \cdot d}. \quad (14)$$

This expression is exactly the one determined by Slonczewski,¹³ i.e., a pure cosine dependence. However, this pure dependence results from an approximation and the precision of this approximation will be discussed in Sec. IV.

It is more interesting to consider the case of a spin dependent ‘‘barrier.’’ This situation includes for example ferro-

magnetic metals inserted between two tunnel barriers (double MTJs (Ref. 27) or quantum wells) and ferromagnetic insulator.²⁸

If we consider that the quantification axis in the barrier is the same as the R electrode, the transfer matrix has the general form

$$\begin{pmatrix} \cos\frac{\theta}{2} & 0 & \sin\frac{\theta}{2} & 0 \\ 0 & \cos\frac{\theta}{2} & 0 & \sin\frac{\theta}{2} \\ -\sin\frac{\theta}{2} & 0 & \cos\frac{\theta}{2} & 0 \\ 0 & -\sin\frac{\theta}{2} & 0 & \cos\frac{\theta}{2} \end{pmatrix} \begin{pmatrix} \alpha_{\uparrow} & \beta_{\uparrow} & 0 & 0 \\ \gamma_{\uparrow} & \delta_{\uparrow} & 0 & 0 \\ 0 & 0 & \alpha_{\downarrow} & \beta_{\downarrow} \\ 0 & 0 & \gamma_{\downarrow} & \delta_{\downarrow} \end{pmatrix}. \quad (15)$$

The exact angular dependence in that case is quite complicated but it is interesting to note that it has the same general expression as expression (9) i.e.,

$$G = D_{\rightarrow}^{\uparrow} + D_{\rightarrow}^{\downarrow} = g_0 \frac{1 + a \cdot \cos \theta}{1 + b \cdot \cos \theta + c \cdot \cos^2 \theta}. \quad (16)$$

This form is also valid in the more general case in which L and R electrodes are different.

Just as previously, we can consider the low attenuation limit for the case of a ferromagnetic insulator (different barrier heights for up and down spin). The two submatrices are thus given by:

$$\begin{pmatrix} \alpha_{\sigma} & \beta_{\sigma} \\ \gamma_{\sigma} & \delta_{\sigma} \end{pmatrix} = \begin{pmatrix} \cosh(q_{\sigma} \cdot d) & -\frac{m'_{\sigma}}{q_{\sigma}} \sinh(q_{\sigma} \cdot d) \\ -\frac{q_{\sigma}}{m'_{\sigma}} \sinh(q_{\sigma} \cdot d) & \cosh(q_{\sigma} \cdot d) \end{pmatrix} \\ \approx \frac{1}{2} \begin{pmatrix} 1 & -\frac{m'_{\sigma}}{q_{\sigma}} \\ -\frac{q_{\sigma}}{m'_{\sigma}} & 1 \end{pmatrix} e^{q_{\sigma} \cdot d}. \quad (17)$$

Then the contribution to the current has the following form:

$$G = 32 \frac{\left[e^{-2q_{\downarrow} \cdot d} \frac{q_{\downarrow}^2 k_{\downarrow}}{m_{\downarrow}'^2 m_{\downarrow}} \left(\frac{k_{\uparrow}^2}{m_{\uparrow}^2} + \frac{q_{\uparrow}^2}{m_{\uparrow}'^2} \right) \left(\frac{k_{\uparrow} k_{\downarrow}}{m_{\uparrow} m_{\downarrow}} + \frac{q_{\uparrow}^2}{m_{\uparrow}'^2} \right) + e^{-2q_{\uparrow} \cdot d} \frac{q_{\uparrow}^2 k_{\uparrow}}{m_{\uparrow}'^2 m_{\uparrow}} \left(\frac{k_{\downarrow}^2}{m_{\downarrow}^2} + \frac{q_{\downarrow}^2}{m_{\downarrow}'^2} \right) \left(\frac{k_{\uparrow} k_{\downarrow}}{m_{\uparrow} m_{\downarrow}} + \frac{q_{\downarrow}^2}{m_{\downarrow}'^2} \right) \right] \left(\frac{k_{\uparrow} + k_{\downarrow}}{m_{\uparrow} + m_{\downarrow}} \right) + \left[e^{-2q_{\downarrow} \cdot d} \frac{q_{\downarrow}^2 k_{\downarrow}}{m_{\downarrow}'^2 m_{\downarrow}} \left(\frac{k_{\uparrow}^2}{m_{\uparrow}^2} + \frac{q_{\uparrow}^2}{m_{\uparrow}'^2} \right) \left(\frac{k_{\uparrow} k_{\downarrow}}{m_{\uparrow} m_{\downarrow}} - \frac{q_{\uparrow}^2}{m_{\uparrow}'^2} \right) - e^{-2q_{\uparrow} \cdot d} \frac{q_{\uparrow}^2 k_{\uparrow}}{m_{\uparrow}'^2 m_{\uparrow}} \left(\frac{k_{\downarrow}^2}{m_{\downarrow}^2} + \frac{q_{\downarrow}^2}{m_{\downarrow}'^2} \right) \left(\frac{k_{\uparrow} k_{\downarrow}}{m_{\uparrow} m_{\downarrow}} + \frac{q_{\downarrow}^2}{m_{\downarrow}'^2} \right) \right] \left(\frac{k_{\uparrow} - k_{\downarrow}}{m_{\uparrow} - m_{\downarrow}} \right) \cos \theta}{\left(\frac{k_{\uparrow}^2}{m_{\uparrow}^2} + \frac{q_{\uparrow}^2}{m_{\uparrow}'^2} \right) \left(\frac{k_{\downarrow}^2}{m_{\downarrow}^2} + \frac{q_{\downarrow}^2}{m_{\downarrow}'^2} \right) \left[4 \frac{k_{\uparrow}^2 k_{\downarrow}^2}{m_{\uparrow}^2 m_{\downarrow}^2} + 2 \frac{k_{\uparrow} k_{\downarrow}}{m_{\uparrow} m_{\downarrow}} \left(\frac{q_{\uparrow}}{m_{\uparrow}'} - \frac{q_{\downarrow}}{m_{\downarrow}'} \right)^2 + 4 \frac{q_{\uparrow}^2 q_{\downarrow}^2}{m_{\uparrow}'^2 m_{\downarrow}'^2} + \left(\frac{k_{\uparrow}^2}{m_{\uparrow}^2} + \frac{k_{\downarrow}^2}{m_{\downarrow}^2} \right) \left(\frac{q_{\uparrow}}{m_{\uparrow}'} + \frac{q_{\downarrow}}{m_{\downarrow}'} \right)^2 - 2 \left(\frac{k_{\uparrow}^2}{m_{\uparrow}^2} - \frac{k_{\downarrow}^2}{m_{\downarrow}^2} \right) \left(\frac{q_{\uparrow}^2}{m_{\uparrow}'^2} - \frac{q_{\downarrow}^2}{m_{\downarrow}'^2} \right) \cos \theta + \left(\frac{k_{\uparrow} - k_{\downarrow}}{m_{\uparrow} - m_{\downarrow}} \right)^2 \left(\frac{q_{\uparrow}}{m_{\uparrow}'} - \frac{q_{\downarrow}}{m_{\downarrow}'} \right)^2 \cos^2 \theta} \right)}. \quad (18)$$

It is obvious from this expression that in the case of a ferromagnetic insulator the angular dependence is intrinsically different from a normal insulator and is not purely cosine. The deviation from the cosine dependence might thus be considered as an indication of presence of spin-filtering. In order to quantify the expected effect, we shall evaluate it numerically. This is shown in Sec. IV.

IV. NUMERICAL COMPUTATIONS

The preceding conclusions have been drawn considering the low transmission limit and only two states at the Fermi level, having a longitudinal wave vector (P to the current flow and perpendicular to the interfaces) contributing significantly to the current. However an accurate estimation of the current requires taking into account the contribution of all the states with their real transmission coefficient. The need to take into account the reduced effective electron mass inside

the barrier, the shape of the barrier and also the tunneling of electrons with nonzero transverse wave vector has been discussed in Ref. 22.

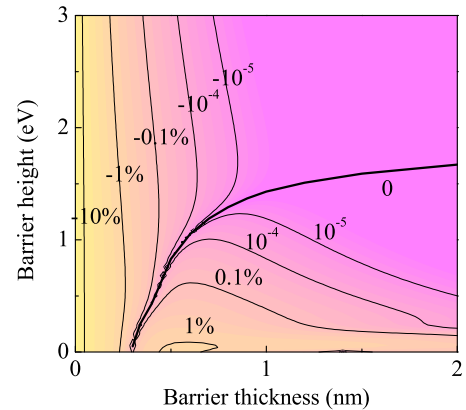


FIG. 2. (Color online) G_2/G_1 ratio for a rectangular normal barrier with an as a function of the barrier thickness and height.

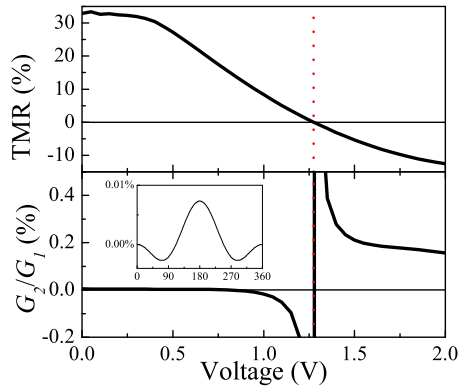


FIG. 3. (Color online) Evolution of the MR (a) and of the G_2/G_1 ratio as a function of the voltage applied to the junction. Barrier parameters are a thickness of 1 nm, a height of 1 eV and an effective mass of $0.4 m_e$. In inset: Angular MR $\{TMR=[R(\theta)-R(0)]/R(0)\}$ at a bias of 1.275 V.

This approach appeared to be particularly relevant to describe experimental evolutions of the MR with voltage in systems made of composite barriers^{22,29,30} or ferromagnetic barriers.^{28,31}

In the case of noncollinear magnetizations configurations, the formalism of current calculation is not changed and the extension of the Tsu–Esaki formula²¹ proposed in Refs. 22 and 32 remains valid. In the zero-temperature limit, the tunnel current density for a spin direction is expressed as

$$J = \frac{2\pi \cdot m_1 \cdot e}{h^3} \left[\int_0^{E_F - eV} \int_{E_F - eV - E_z}^{E_F - E_z} D(E_z, E_{\parallel}) dE_{\parallel} \cdot dE_z + \int_{E_F - eV}^{E_F} \int_0^{E_F - E_z} D(E_z, E_{\parallel}) dE_{\parallel} \cdot dE_z \right].$$

The transmission coefficient is thus numerically integrated over E_{\parallel} and E_z for each spin direction to get the total tunnel current. Note that expression (8) of the transmission coefficient is only valid if a propagating state exists for each spin direction in each electrode. Similar expressions have been established for the other cases by considering evanescent waves in the electrodes.

The numerical parameters used in the following calculations have been chosen to reflect real systems.²² The effective mass of the electron in the barrier regions is equal to 0.4 times the free-electron mass. The electrodes parameters are the ones proposed by Davies and MacLaren.³³ The Fermi level is 2.25 eV (0.35 eV) and the effective mass is 1.27 (1.36) the mass of the free-electron for spin up (respectively, for spin down) band. These parameters correspond to an intrinsic polarization of 42%. They are kept constant in the following calculations. Nevertheless the general trend of increased deviation from the cosine dependence with the intrinsic polarization mentioned earlier for the δ barrier is confirmed by numerical calculation for square barriers.

Figure 2 represent the G_2/G_1 ratio for a rectangular single nonmagnetic tunnel barrier. The deviation of the angular dependence from the cosine dependence is very weak and gets significant (over 1%) only for barrier thicknesses below 0.3 nm. For the barriers encountered in common devices, the deviation is thus completely negligible at low bias

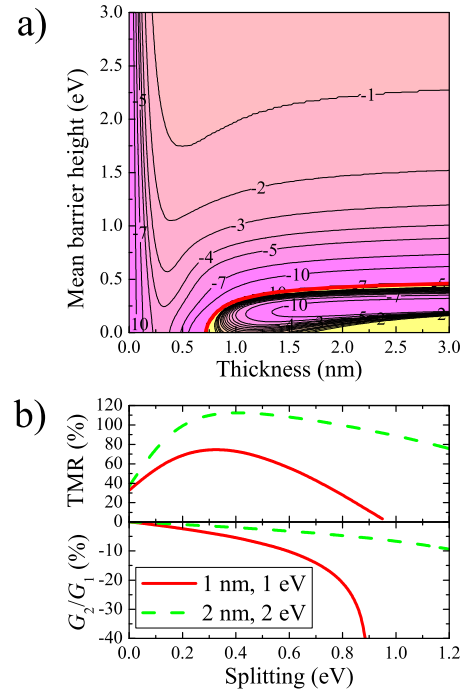


FIG. 4. (Color online) (a) G_2/G_1 ratio for a rectangular ferromagnetic barrier as a function of the barrier thickness d and mean height $\bar{\varphi}$. The effective mass is $0.4 m_e$ and the difference between spin up and down bands is 0.25 eV. (b) Influence of the splitting Δ in the barrier on the MR and on the G_2/G_1 ratio for two sets of parameters: $d=1$ nm and $\bar{\varphi}=1$ eV (red line) and $d=2$ nm and $\bar{\varphi}=2$ eV (green line)

and the cosine dependence of the conductance given by Slonczewski in the low penetration limit holds.

This low penetration approximation might be further questionable at high biases. Here the electric field reduces the average barrier height. It is well known that the MR of conventional MTJs decreases with the voltage. This decrease can be due to several factors like bands structure or inelastic tunneling. The parabolic band model is particularly efficient in describing the effect of tunnel barrier deformation at high bias.²² As already mentioned, the MR ratio reflects only the conduction in the P and AP state. As this MR decreases, the relative importance of the second order term might increase. As represented in Fig. 3, it is indeed the case for a conventional tunnel barrier (1 nm thick, 1 eV high). At high bias, this relative part gets beyond 0.1%. For a precise voltage at which the MR is close to zero, the second order component is clearly visible as shown in inset of Fig. 3.

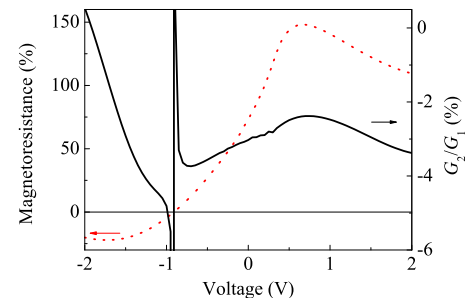


FIG. 5. (Color online) Evolution of the MR (dotted line) and of the G_2/G_1 ratio (continuous line) as a function of the voltage applied to the junction. Barrier parameters are a thickness of 1 nm, a height of 1 eV, effective mass of $0.4 m_e$ and splitting of 0.25 eV.

At high bias, the second order term of the angular dependence remains very small but still could be measured. However highlighting the existence of such a second order term is an experimental challenge since it would require a perfect control of the angle between the magnetization (including the influence of the current going through the junction) and to rule out any TAMR effect.

The previous numerical calculations show that the cosine dependence of the MR established in the low penetration limit is a very good approximation for a non magnetic barrier. Previously, we saw that in the low penetration limit, the angular dependence of conductance for a ferromagnetic barrier is expected to differ significantly from cosine. We shall now confirm this point numerically.

For a ferromagnetic barrier, two different barrier heights, $\bar{\varphi} + \Delta$ and $\bar{\varphi} - \Delta$, are considered, respectively, for down and up spins. Δ represents the splitting due to the exchange interaction within the insulator or semiconductor. To our knowledge, the maximum reported value for this splitting is 0.25 eV for EuO.³⁴

Figure 4(a) represents the G_2/G_1 ratio for a MTJ with a ferromagnetic barrier as a function of its thickness and its mean barrier height $\bar{\varphi}$. The exchange splitting is kept constant to a value $\Delta = 0.25$ eV.

Significant G_2/G_1 ratios over several percents are obtained in a wide range of parameters. The ratio increases for lower barrier height but does not vary much as the barrier thickness increases. Exact numerical computations confirm the qualitative conclusions of Sec. III: the angular dependence of the MR in structure including a ferromagnetic insulator differs intrinsically from normal MTJs. This effect is directly linked to the existence of the splitting of the bands in the barrier and increases with the splitting as shown in Fig. 4(b). The decrease in MR observed for high splitting in Fig. 4(b) is somehow counter intuitive. For high splittings, the difference of transmission for the two spin directions is so high that the conduction proceeds nearly entirely by the spin up band in the barrier. The MR is, therefore, ruled by the polarization in the electrode rather than by the difference in barrier heights within the barrier.

The evolution of MR with voltage in spin-filtering MTJs exhibits particular features.^{28,35} The parabolic band model is only partly relevant to explain these features. In Fig. 5 a typical MR(V) curve for a spin filter junction³¹ is reported. The G_2/G_1 ratio is of several percent over a wide voltage range. As it is the case for normal barrier at voltages for which the MR is close to zero, the second order term can be dominant.

V. CONCLUSION

In this paper, we present a simple formalism to investigate the angular evolution of arbitrary ballistic structures in the parabolic band model. Using analytic expressions in the low penetration limit, we evidenced an intrinsic difference between normal and ferromagnetic barriers. For normal barriers, the conductance exhibits a purely cosine dependence as a function of the angle between the magnetizations whereas for ferromagnetic barriers the angular dependence is more complex.

These conclusions have been further supported by numerical evaluation of the conductance based on exact transmission coefficients and taking into account all the states. For normal barriers, the deviation from the cosine dependence is negligible for realistic parameters. On the contrary, for spin-filtering junctions including a ferromagnetic barrier, the deviation from the cosine dependence can be of several percents of the MR.

Beyond the simple MR ratio which is based on the two extreme configurations of the magnetizations (P and AP), the angular dependence of the MR can thus give more insight in the transport phenomena. Of course the deviations to the cosine dependence being small, the exact characterization of the angular dependence remains an experimental challenge since the magnetic configurations have to be well controlled. Note that the precessional motion of magnetization excited by spin transfer torque is also a measure of the angular dependence of the MR. Any deviation from the exact cosine dependence might influence the harmonic spectrum.

APPENDIX

In the whole heterostructure, both the total energy E and the transverse wave vector k_{\parallel} are conserved. It is important to note that as the effective mass varies along the structure, the transverse and longitudinal part of the energy are not in general conserved independently and $E_z = E - [\hbar^2/2m(z)]k_{\parallel}^2$. Being a linear second order differential equation, the unidimensional Schrödinger equation $\partial^2 \varphi(z)/\partial z^2 + 2m/\hbar^2 [E_z - V(z)]\varphi(z) = 0$ admits general solutions of the form $\varphi(z) = A \cdot f(z) + B \cdot g(z)$, f and g being defined by $V(z)$ and E_z . As the two parameters can be deduced from the value of the wave function and its derivative at one point, it is possible to establish a linear relation between two arbitrary points of the form

$$\begin{pmatrix} \varphi(z_1) \\ \varphi'(z_1)/m \end{pmatrix} = \begin{pmatrix} \alpha & \beta \\ \gamma & \delta \end{pmatrix} \begin{pmatrix} \varphi(z_2) \\ \varphi'(z_2)/m \end{pmatrix},$$

with

$$\begin{pmatrix} \alpha & \beta \\ \gamma & \delta \end{pmatrix} = \begin{pmatrix} f(z_1) \cdot g'(z_2) - f'(z_2) \cdot g(z_1) & m(f(z_2) \cdot g(z_1) - f(z_1) \cdot g(z_2)) \\ \frac{1}{m}(f'(z_1) \cdot g'(z_2) - f'(z_2) \cdot g'(z_1)) & f(z_2) \cdot g'(z_1) - f'(z_1) \cdot g(z_2) \end{pmatrix}.$$

Determining this “transfer matrix” in regions with linear variation of the potential is trivial, as the solutions of the Schrödinger equation are analytic. For a constant potential $V(z) = V_0$, the wave function is a simple linear combination of real or imaginary exponentials so that for a region of thickness d , the 2×2 submatrixes are given by

$$\begin{aligned}
 E_z > V_0 \quad k &= \sqrt{\frac{2m}{\hbar^2}(E_z - V_0)} \begin{pmatrix} \cos(k \cdot d) & -\frac{m}{k}\sin(k \cdot d) \\ \frac{k}{m}\sin(k \cdot d) & \cos(k \cdot d) \end{pmatrix} \\
 E_z = V_0 & \begin{pmatrix} 1 & -m \cdot d \\ 0 & 1 \end{pmatrix} \\
 E_z < V_0 \quad q &= \sqrt{\frac{2m}{\hbar^2}(V_0 - E_z)} \begin{pmatrix} \cosh(q \cdot d) & -\frac{m}{q}\sinh(q \cdot d) \\ -\frac{q}{m}\sinh(q \cdot d) & \cosh(q \cdot d) \end{pmatrix}
 \end{aligned}$$

In the limit of low thickness and infinite V_0 , it is possible to consider similarly a δ barrier $V(z) = (\hbar^2/2)\gamma \cdot \delta(z)$ with the following submatrix: $\begin{pmatrix} 1 & 0 \\ \gamma & 1 \end{pmatrix}$

For a region with a linear variation in the potential $V(z) = V_0 + F \cdot z$, the wave function can be written in terms of Airy functions

$$\begin{pmatrix} \frac{\varphi(z_1)}{m} \\ \frac{\varphi'(z_1)}{m} \end{pmatrix} = \pi \begin{pmatrix} \text{Ai}(\rho_1) \cdot \text{Bi}'(\rho_2) - \text{Ai}'(\rho_2)\text{Bi}(\rho_1) & \sqrt{\frac{m^2 \cdot \hbar^2}{2F}} (\text{Ai}(\rho_2) \cdot \text{Bi}(\rho_1) - \text{Ai}(\rho_1) \cdot \text{Bi}(\rho_2)) \\ \sqrt{\frac{2F}{m^2 \cdot \hbar^2}} (\text{Ai}'(\rho_1)\text{Bi}'(\rho_2) - \text{Ai}'(\rho_2)\text{Bi}'(\rho_1)) & \text{Ai}(\rho_2)\text{Bi}'(\rho_1) - \text{Ai}'(\rho_1)\text{Bi}(\rho_2) \end{pmatrix} \begin{pmatrix} \frac{\varphi(z_2)}{m} \\ \frac{\varphi'(z_2)}{m} \end{pmatrix},$$

with $\rho_{1,2} = (2m/\hbar^2 \cdot F^2)^{1/2} [V(z_{1,2}) - E_z]$

Note that the divergence of the Airy potentials (low F), it is thus necessary to use in that case asymptotic forms of the Airy functions.

If the potential between the two electrodes of the tunnel junction can be described in different regions where the potential is constant or varies linearly, the total transfer matrix is simply deduced from multiplication of the simple complex matrixes given above. Whatever the structure is, containing either insulating or conducting layers, it is totally described by three coefficients (the four coefficients are linked by the property of the transfer matrix which has a determinant of 1).

¹S. A. Wolf, *J. Supercond.* **13**, 195 (2000); J. M. Daughton, *J. Appl. Phys.* **81**, 3758 (1997); W. J. Gallagher, J. H. Kaufman, S. S. P. Parkin, and R. E. Scheuerlin, U. S. Patent No. 5,640,343, June, 17 (1997).

²J. S. Moodera, L. R. Kinder, T. M. Wong, and R. Meservey, *Phys. Rev. Lett.* **74**, 3273 (1995).

³J. Faure-Vincent, C. Tiusan, E. Jouguelet, F. Canet, M. Sajieddine, C. Bellouard, E. Popova, M. Hehn, F. Montaigne, and A. Schuhl, *Appl. Phys. Lett.* **82**, 4507 (2003).

⁴C. Tiusan, M. Sicot, J. Faure-Vincent, M. Hehn, C. Bellouard, F. Montaigne, S. Andrieu, and A. Schuhl, *J. Phys.: Condens. Matter* **18**, 941 (2006).

⁵S. S. P. Parkin, C. Kaiser, A. Panchula, P. M. Rice, B. Hughes, M. Samant, and S.-H. Yang, *Nature Mater.* **3**, 862 (2004).

⁶S. Yuasa, A. Fukushima, T. Nagahama, K. Ando, and Y. Suzuki, *Jpn. J. Appl. Phys., Part 1* **43**, L588 (2004); D. D. Djayaprawira, K. Tsunekawa, M. Nagai, H. Maehara, S. Yamagata, N. Watanabe, S. Yuasa, Y. Suzuki, and K. Ando, *Appl. Phys. Lett.* **86**, 092502 (2005).

⁷S. Ikeda, J. Hayakawa, Y. Ashizawa, Y. M. Lee, K. Miura, H. Hasegawa, M. Tsunoda, F. Matsukura, and H. Ohno, *Appl. Phys. Lett.* **93**, 082508 (2008).

⁸A. Brataas, G. E. W. Bauer, and P. J. Kelly, *Phys. Rep.* **427**, 157 (2006).

⁹L. Berger, *J. Appl. Phys.* **49**, 2156 (1978); **55**, 1954, (1984).

¹⁰J. Slonczewski, *J. Magn. Magn. Mater.* **159**, L1 (1996); **195**, L261 (1999).

¹¹S. Urazhdin, R. Loloee, and W. P. Pratt, *Phys. Rev. B* **71**, 100401(R)

(2005) and references therein.

¹²G. E. W. Bauer, Y. Tserkovnyak, D. Huertas-Hernando, and A. Brataas, *Phys. Rev. B* **67**, 094421 (2003).

¹³J. C. Slonczewski, *Phys. Rev. B* **39**, 6995 (1989).

¹⁴H. Jaffrès, D. Lacour, F. Nguyen Van Dau, J. Briatico, F. Petroff, and A. Vaurès, *Phys. Rev. B* **64**, 064427 (2001).

¹⁵L. Gao, X. Jiang, S.-H. Yang, J. D. Burton, E. Y. Tsymlal, and S. S. P. Parkin, *Phys. Rev. Lett.* **99**, 226602 (2007).

¹⁶C. Tiusan, J. Faure-Vincent, C. Bellouard, M. Hehn, E. Jouguelet, and A. Schuhl, *Phys. Rev. Lett.* **93**, 106602 (2004).

¹⁷M. Braun, J. König, and J. Martinek, *Phys. Rev. B* **70**, 195345 (2004).

¹⁸Y.-Q. Zhou, R.-Q. Wang, B. Wang, and D. Y. Xing, *Phys. Rev. B* **76**, 075343 (2007).

¹⁹H. Zhang, G.-M. Zhang, and L. Yu, *J. Phys.: Condens. Matter* **21**, 155501 (2009) and references therein.

²⁰F. Montaigne, M. Hehn, and A. Schuhl, *J. Appl. Phys.* **91**, 7020 (2002).

²¹R. Tsu and L. Esaki, *Appl. Phys. Lett.* **22**, 562 (1973).

²²F. Montaigne, M. Hehn, and A. Schuhl, *Phys. Rev. B* **64**, 144402 (2001).

²³G. E. Blonder, M. Tinkham, and T. M. Klapwijk, *Phys. Rev. B* **25**, 4515 (1982).

²⁴Y. Qi, D. Y. Xing, and J. Dong, *Phys. Rev. B* **58**, 2783 (1998).

²⁵Z. Zheng, Y. Qi, D. Y. Xing, and J. Dong, *Phys. Rev. B* **59**, 14505 (1999).

²⁶H. B. Heersche, Th. Schäpers, J. Nitta, and H. Takayanagi, *Phys. Rev. B* **64**, 161307 (2001).

²⁷G. Feng, S. van Dijken, and J. M. D. Coey, *Appl. Phys. Lett.* **89**, 162501 (2006).

²⁸T. Nagahama, T. S. Santos, and J. S. Moodera, *Phys. Rev. Lett.* **99**, 016602 (2007).

²⁹L. Le Brizoual, P. Alnot, M. Hehn, F. Montaigne, M. Alnot, A. Schuhl, and E. Snoeck, *Appl. Phys. Lett.* **86**, 112505 (2005).

³⁰C. de Buttet, M. Hehn, F. Montaigne, C. Tiusan, G. Malinowski, A. Schuhl, E. Snoeck and S. Zoll, *Phys. Rev. B* **73**, 104439 (2006).

³¹A. Saffarzadeh, *J. Magn. Magn. Mater.* **269**, 327 (2004).

³²S. S. Liu and G. Y. Guo, *J. Magn. Magn. Mater.* **209**, 135 (2000).

³³A. Davis and J. Maclaren, *J. Appl. Phys.* **87**, 5224 (2000).

³⁴J. S. Moodera, T. S. Santos, and T. Nagahama, *J. Phys.: Condens. Matter* **19**, 165202 (2007).

³⁵U. Lüders, M. Bibes, S. Fusil, K. Bouzehouane, E. Jacquet, C. B. Sommers, J.-P. Contour, J.-F. Bobo, A. Barthélémy, A. Fert, and P. M. Levy, *Phys. Rev. B* **76**, 134412 (2007).